Degenerate Ground State and Anomalous Flux Hysteresis in an $YBa_2Cu_3O_7$ Grain Boundary r.f. SQUID

C H Gardiner[1]†, R A M Lee[2], J C Gallop[1], A Ya Tzalenchuk[1], J C Macfarlane[3] and L Hao[1]

[1]National Physical Laboratory, Queens Road, Teddington, Middlesex, TW11 0LW, UK
[2]California Institute of Technology, Condensed Matter Physics, Mail Code 114-36, 1251 E. California Blvd., Pasadena, CA 91125, USA
[3]Department of Physics, University of Strathclyde, Glasgow, G4 0NG, UK

Abstract. We report measurements of the flux hysteresis curves and trapped flux distribution in an $YBa_2Cu_3O_7$ r.f. SQUID containing two closely spaced grain boundary Josephson junctions in parallel. Broadening of the flux distribution from T = 15 K to 30 K is followed by a bifurcation at T = 35 K which corresponds to a degenerate ground state. Above $T \approx 40$ K the bifurcation disappears, the flux distribution narrows significantly and small secondary loops appear in the hysteresis curves. This behaviour can be modelled qualitatively if we assume a temperature dependent second harmonic term in the current-phase relationship of the junctions.

1. Introduction

In recent years there has been much interest in Josephson junctions and superconducting quantum interference devices (SQUIDs) fabricated from high temperature superconductor (HTS) materials. A series of elegant experiments have utilised the effects of phase continuity in superconducting rings [1, 2, 3] and quantum interference in wide junctions [4, 5, 6] to demonstrate the predominantly $d_{x^2-y^2}$-wave symmetry of the order parameter.

It has been shown that it is possible to trap half flux quanta in rings containing an odd number of "π-junctions" [2]. A π-junction is so called because in its ground state the phase change of the order parameter across it is π. This occurs when the current-phase relationship (CPR) is inverted (i.e. the critical current becomes negative) — an effect that occurs in junctions between two superconductors of $d_{x^2-y^2}$-wave symmetry when their crystal axes are misaligned by more than 45° [7]. Such junctions can be created by a number of techniques, including the use of HTS grain boundaries.

It has also been shown that the CPR in HTS junctions is non-sinusoidal, possessing a second harmonic component whose magnitude depends on the relative orientation of the $d_{x^2-y^2}$-wave superconductors [8], and whose sign can be temperature dependent [9]. For a junction contained in a SQUID ring, the CPR can be expanded as a Fourier series in ϕ, the phase difference of the superconducting order parameter across the junction:

$$I = I_{c1}\sin(\phi) + I_{c2}\sin(2\phi) + \ldots, \tag{1}$$

where I is the supercurrent flowing through the junction. In an asymmetric 45° [001]-tilt grain boundary junction between two $d_{x^2-y^2}$-wave superconductors, the first harmonic I_{c1} is expected to disappear by symmetry [7] (although in practice it does not disappear completely,

† To whom correspondence should be addressed (Before 1 May 2004: carol.gardiner@npl.co.uk; After 1 May 2004: carol.webster@npl.co.uk).

due to microscopic or nanoscale faceting of the boundary [10]). The second harmonic I_{c2} then becomes prominent, and has been observed in recent studies [11, 12].

In this paper we present measurements of the distribution of trapped flux and of the flux hysteresis curves in an $YBa_2Cu_3O_7$ SQUID containing asymmetric 30° [001]-tilt grain boundary junctions. Our observations appear to indicate the presence of a temperature dependent second harmonic term.

2. Device fabrication

The device consists of a thin film of $YBa_2Cu_3O_7$ (~ 200 nm thick), grown by pulsed laser deposition on a $SrTiO_3$ bi-crystal substrate with a well-defined asymmetric misorientation angle of 30°. It was originally designed as a potential dissipationless noise thermometer [13, 14], and therefore consists of a large square washer (6 mm × 8 mm) interrupted by two closely spaced grain boundary junctions in parallel (5 μm × 3 μm). A small control loop is positioned close to the junctions to allow external flux to be applied. Figure 1 shows a schematic diagram of the device. The incorporation of two parallel junctions is historical, and is irrelevant to the work described in this paper. Since the loop enclosed by the junctions is tiny in comparison to the main washer loop, and hence has negligible self inductance, we will treat the pair as a single junction. The other Josephson junction formed by the grain boundary on the wide part of the washer loop has a very large critical current, and can therefore be ignored. Hence, we have an r.f. SQUID consisting of a washer effectively interrupted by a single grain boundary junction.

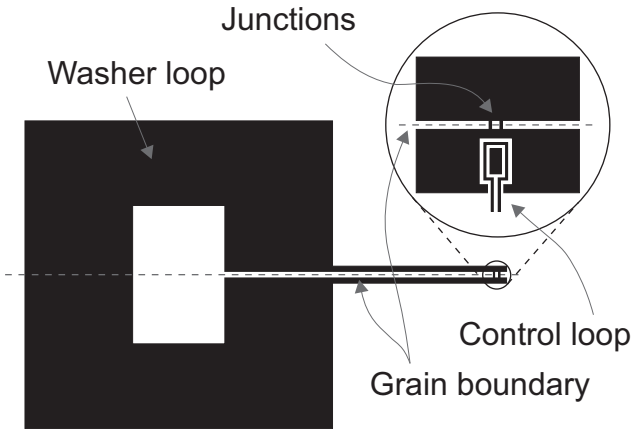

Figure 1. Schematic diagram of washer and Josephson junctions (not to scale). The control loop is used to provide external magnetic flux.

3. Experimental details

A schematic diagram of the experimental setup is shown in Figure 2. Inside an evacuated glass canister the device was mounted on the end of a sapphire rod in thermal contact with the cold finger of a continuous flow He siphon. Temperature control was achieved by passing high frequency a.c. current‡ through a wire wound heater. A separate d.c. readout SQUID was positioned outside the glass, 6 mm from the r.f. SQUID and well inductively coupled. The whole system was immersed in a bath of liquid nitrogen.

‡ A low pass filter on the readout SQUID was used to filter out any stray fields from the heater coil.

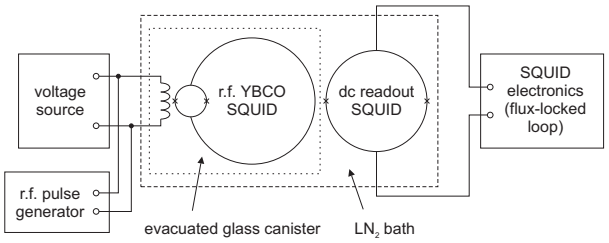

Figure 2. Schematic diagram of the experimental setup.

4. Results

The flux hysteresis curves were measured by slowly sweeping the d.c. current through the control loop at each set temperature. The internal flux threading the washer was monitored by the readout SQUID, which was operated in flux-locked mode. The measurements are displayed in Figure 3. We have estimated the linear background arising from coupling of the external applied field into the readout SQUID, and subtracted this from each plot.

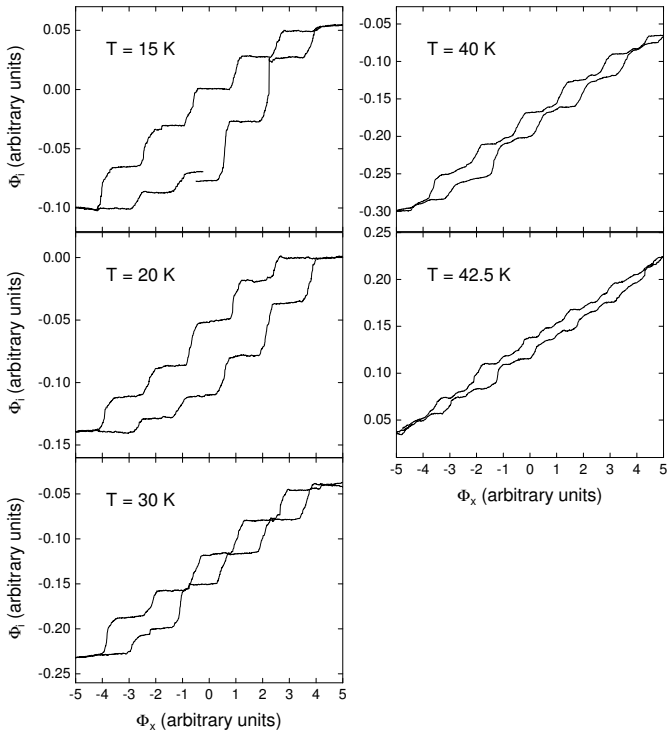

Figure 3. Temperature dependence of hysteresis curves. Small secondary loops appear at $T \geq 40\,\mathrm{K}$.

The data show discrete steps in the internal flux, which we interpret as the admission of individual flux quanta into the washer loop. However, the hysteresis curves do not correspond to those of an ideal SQUID. At temperatures of 15 K, 20 K and 30 K the steps are not all exactly equal in height. Some, particularly those at the extreme ends of the field sweep, appear to be approximately half the average size, suggesting that the washer sometimes admits half flux quanta. At 40 K small steps in the internal flux begin to appear alongside the larger

steps seen at lower temperatures. The alternation of large and small steps causes secondary loops to appear between the main loops of the hysteresis curves. The half-sized steps evident at $T = 15\,\mathrm{K}$ to $T = 20\,\mathrm{K}$ and the secondary loops at $T \geq 40\,\mathrm{K}$ are suggestive of a second harmonic component in the CPR. At 42.5 K the secondary loops increase in size, suggesting an increase in the importance of the second harmonic.

To sample the internal flux distribution we applied a series of r.f. pulses to the control loop and used the readout SQUID to monitor the internal flux threading the washer. The principle behind this procedure is as follows. By carefully tuning the amplitude and frequency of the r.f. signal it is possible to suppress the critical currents of the junctions through the a.c. Josephson effect. Therefore, during a high r.f. pulse, the potential barriers between the metastable flux states of the ring are lowered, and the flux can fluctuate classically. During a low pulse, the barriers are restored and the flux is trapped in a metastable quantised state. Thus, a succession of high and low r.f. pulses causes the internal flux threading the washer loop to be repeatedly trapped and released. By recording the signal from the readout SQUID during each low r.f. pulse a histogram of flux states can be built up.

To achieve the r.f. amplitude and frequency required to suppress the junction critical currents we applied a continuous r.f. signal while measuring the flux hysteresis curves. When discrete flux jumps no longer occurred we were able to deduce that the critical currents were suppressed. We then applied a series of r.f. pulses at each set temperature and recorded the internal flux state of the washer using the readout SQUID, the response of which we binned into histograms.

From the low temperature hysteresis curves we were able to determine the change in the readout SQUID signal brought about by admission of a single flux quantum to the washer loop. This allowed us to put the histograms on an absolute flux scale. We then normalised the data to an area of 1 for comparison with theory. Figure 4 shows the measured flux distibution at a series of temperatures.

The flux distribution is observed to broaden considerably from a width of $0.21\Phi_0$ at 15 K to $0.5\Phi_0$ at 30 K. It then suddenly bifurcates at $T = 35\,\mathrm{K}$. The peaks of the bifurcated distribution are separated by $0.5\Phi_0$ at 35 K, which clearly indicates the presence of a strong second harmonic in the CPR. At 37.5 K the peaks are separated by $0.3\Phi_0$, which suggests a decline in the contribution of the second harmonic. At $T = 40\,\mathrm{K}$ the flux distribution suddenly reverts to a single peak and becomes much narrower than at lower temperatures.

5. Modelling

In this section we model the flux hysteresis curves and the flux distribution, assuming a single Josephson junction and taking into account the possibility of a second harmonic term in the CPR.

The internal flux threading a superconducting ring is given by

$$\Phi_\mathrm{i} = \Phi_\mathrm{x} + IL, \tag{2}$$

where Φ_x is the external applied flux, I is the supercurrent and L is the self-inductance of the ring. The supercurrent can be obtained from the CPR (1). The requirement of phase continuity around a superconducting ring gives rise to the condition $\phi + \frac{2\pi\Phi_\mathrm{i}}{\Phi_0} = 2n\pi$ (quantisation of the fluxoid [16]). If we substitute this into (1) we obtain

$$I = -I_{\mathrm{c}1}\sin\left(\frac{2\pi\Phi_\mathrm{i}}{\Phi_0}\right) - I_{\mathrm{c}2}\sin\left(\frac{4\pi\Phi_\mathrm{i}}{\Phi_0}\right) - \ldots. \tag{3}$$

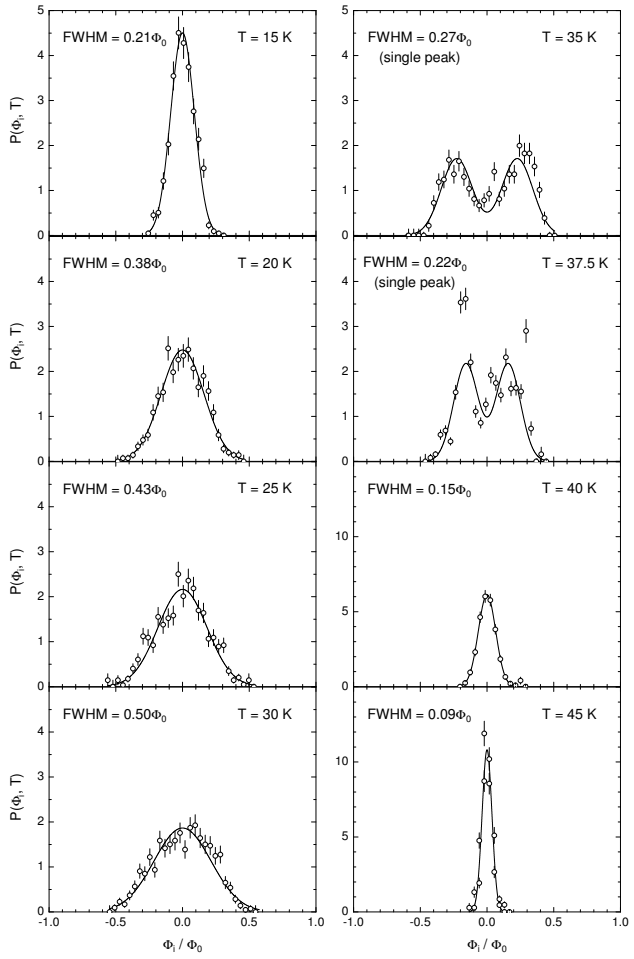

Figure 4. Temperature dependence of flux distribution. The open circles are the normalised histogram data and the lines are gaussian fits using one or two gaussians. The distribution bifurcates at $T = 35\,\mathrm{K}$.

Substituting (3) into (2) and rearranging, we obtain

$$\Phi_\mathrm{x} = \Phi_\mathrm{i} + I_\mathrm{c1} L \sin\left(\frac{2\pi\Phi_\mathrm{i}}{\Phi_0}\right) + I_\mathrm{c2} L \sin\left(\frac{4\pi\Phi_\mathrm{i}}{\Phi_0}\right). \tag{4}$$

Equation (4) allows us to model the hysteresis curves by varying the magnitudes and signs of the parameters I_c1 and I_c2.

We model the flux distribution according to the Boltzmann distribution, so we must first calculate the internal energy of the ring. This is given by

$$U(\Phi_\mathrm{i}, \Phi_\mathrm{x}) = \frac{(\Phi_\mathrm{i} - \Phi_\mathrm{x})^2}{2L} + \int_0^\phi I \,\mathrm{d}\phi, \tag{5}$$

where the first term is the classical free energy of the ring and the second term is the Josephson coupling energy of the junction. Evaluating the integral and again utilising the condition $\phi + \frac{2\pi\Phi_\mathrm{i}}{\Phi_0} = 2n\pi$ we obtain

$$U(\Phi_\mathrm{i}, \Phi_\mathrm{x}) = \frac{(\Phi_\mathrm{i} - \Phi_\mathrm{x})^2}{2L} - \frac{I_\mathrm{c1}\Phi_0}{2\pi}\cos\left(\frac{2\pi\Phi_\mathrm{i}}{\Phi_0}\right) - \frac{I_\mathrm{c2}\Phi_0}{4\pi}\cos\left(\frac{4\pi\Phi_\mathrm{i}}{\Phi_0}\right). \tag{6}$$

This function has metastable minima if I_{c1} and I_{c2} are large enough. The flux distribution is given by

$$P(\Phi_i, \Phi_x, T) = P_0 \exp\left(-\frac{U(\Phi_i, \Phi_x)}{k_B T}\right), \tag{7}$$

where $P(\Phi_i, \Phi_x, T)$ is the normalised probability of finding the ring in flux state Φ_i, at temperature T, given an external flux Φ_x. P_0 is the constant of proportionality (obtained from the condition $\int_{-\infty}^{\infty} P(\Phi_i, \Phi_x, T)\, d\Phi_i = 1$) and k_B is Boltzmann's constant.

By varying the parameters I_{c1}, I_{c2} and L in Equations (4) and (7) we can model the observed flux hysteresis curves and the flux distributions. A wide variety of different behaviour can be reproduced by considering both negative and positive values of I_{c1} and I_{c2}:

- Half-sized steps or secondary loops in the hysteresis curves require I_{c2} to be negative and I_{c1} to be either negative or positive. If both are large, we obtain large hysteresis loops with half-sized steps at the extreme ends. If both are smaller we obtain small hysteresis loops interspersed with even smaller secondary loops.
- A bifurcated flux distribution with peak separation $\leq 0.5\Phi_0$ can be achieved most readily with negative I_{c2}. Negative I_{c1} gives rise to a bifurcation of the flux distribution with peak separation $\leq \Phi_0$.
- A single peak in the flux distribution can be achieved with a wide variety of different parameters. Positive values of I_{c1} and/or I_{c2} result in a narrow peak, whereas small negative values of I_{c1} and/or I_{c2} result in a broad peak. Increasing L increases the peak width for all values of I_{c1} and I_{c2}.

Figure 5 shows simulations of the hysteresis curves which best model the data shown in Figure 3. Figure 6 shows simulations of the flux distributions which best model the data shown in Figure 4. A value of $L = 0.4$ nH was used in the simulations of both the hysteresis curves and the flux distributions, as this ensured insignificant population of higher flux states, in accordance with our observations. We also assumed no external flux to be present.

Qualitative agreement is obtained between measurement and simulation for both the hysteresis curves and the flux distribution. The half-sized steps at the extreme ends of the flux hysteresis curves at $T = 15$ K and $T = 20$ K can be reproduced using negative values for both I_{c1} and I_{c2}. The magnitudes of I_{c1} and I_{c2} decrease with temperature, causing the large hysteresis loops to gradually close up and the secondary loops to appear. The broadening of the flux distribution can be modelled with a value of I_{c2} which starts small and positive, but decreases through zero to become negative for $T \geq 30$ K. At $T = 35$ K and $T = 37.5$ K the bifurcation in the flux distribution is reproduced with much larger negative values of I_{c2}. For $T \geq 40$ K the flux distribution recombines to form a single, narrow peak. This can be reproduced using large positive values of I_{c2}.

Although we have obtained qualitative agreement between the model and the two data sets, we have not been able to find sets of parameters that are consistent with both data sets at all temperatures. Over the temperature range 30–42.5 K we model the hysteresis curves using negative values of I_{c1} and I_{c2}, where I_{c2} increases slightly in magnitude, but I_{c1} decreases. Over the temperature range 35–37.5 K we are able to model the bifurcated flux distributions using very similar parameters. However, outside this temperature range the parameters required to model the single peaks observed in the flux distributions are very different from those used for the hysteresis curves.

Unfortunately no hysteresis curves were measured at $T = 35$ K and $T = 37.5$ K, so the results of the two simulations cannot be compared directly. At $T = 40$ K we do have data for both the hysteresis curve and the flux distribution, but the parameters required to model the

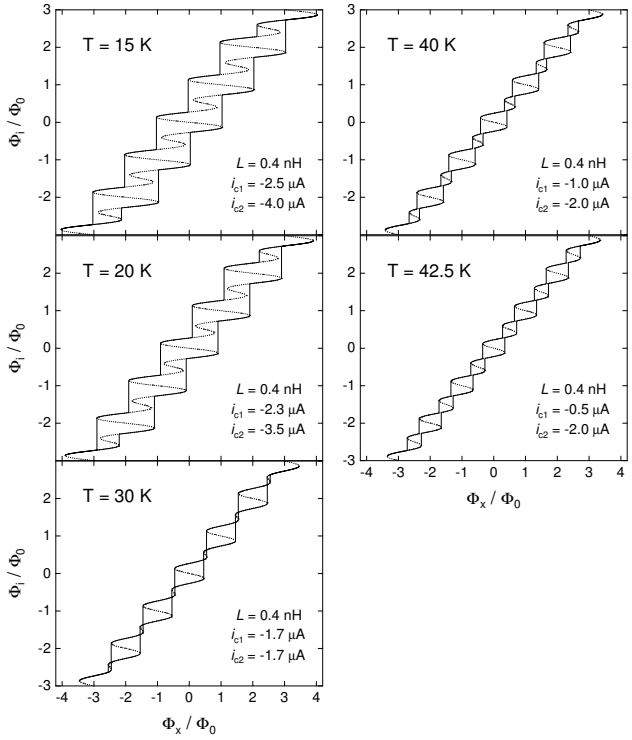

Figure 5. Simulated hysteresis curves (solid lines). The dashed lines show regions of the Φ_i versus Φ_x curve that are inaccessible due to the potential barrier between metastable flux states.

two sets of data are quite different: negative I_{c1} and I_{c2} for the hysteresis curve, but positive I_{c1} and I_{c2} for the flux distribution.

Over the temperature range T = 15–30 K we also have data for both hysteresis curves and flux distributions, but again the parameters used to model these are very different. We also note that our simulations of the hysteresis curves at T = 15 K and T = 20 K contain six flux jumps rather than the five observed. If we had used positive values of I_{c1} rather than negative ones, we would have obtained simulations of almost identical shape, but with five steps.

Figure 7 shows the temperature dependence of the parameters I_{c1} and I_{c2} obtained from the two simulations. The only temperature range over which the two parameter sets agree is 35–37.5 K.

6. Discussion

Before concluding, we will discuss other possible mechanisms which could explain our data. A doubly degenerate ground state, as observed from the bifurcation of the flux distribution, can be obtained by a number of mechanisms. A superconducting ring that contains an odd number of π-junctions is expected to produce a degenerate ground state regardless of the existence of a second harmonic term in the CPR [15]. However, the two degenerate flux states are expected to be separated by $\sim \Phi_0$ in such a ring, whereas we observe a separation of $\sim 0.5\Phi_0$. In order to achieve a separation of $\leq 0.5\Phi_0$ using only a negative I_{c1} we find that the critical current must be very low, leading to a very small potential barrier between the degenerate states, and therefore, poorly resolved flux states. We observe well separated flux states, which can only be modelled using a substantial negative I_{c2}.

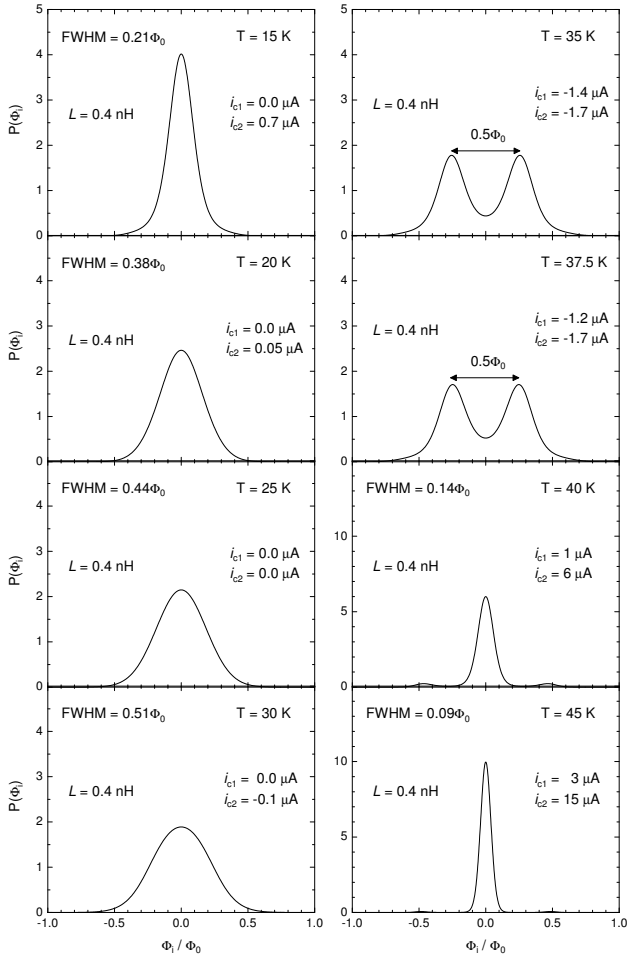

Figure 6. Simulations of the flux distribution. The bifurcation at 35 K can be reproduced with a large negative I_{c2}. The very narrow single peak at $T \geq 40$ K can be reproduced with a large positive I_{c2}.

If we had overestimated by a factor of 2 the response of the readout SQUID to a flux change of Φ_0 in the washer loop, this would mean that the peaks in the bifurcated flux distribution were separated by a factor of Φ_0 rather than $0.5\Phi_0$. However, we feel that this is unlikely since it would mean that the majority of the flux jumps observed in the hysteresis curves were $2\Phi_0$.

The ground state of a superconducting ring is also doubly degenerate in the presence of an external flux of $\Phi_0/2$. However, in such a case the degenerate states are separated by exactly Φ_0, which is not observed. We also think it highly unlikely that any stray external flux should take a value of exactly $\Phi_0/2$. If the stray flux should deviate from this value, we would expect one state to be preferred, but to within experimental uncertainty we observe the two states to be equally populated.

Finally, it is possible that the secondary loops observed in the hysteresis curves are due to the geometry of the r.f. SQUID. It is unfortunate that the historical design incorporated two junctions in parallel rather than one, and we cannot rule out the possibility that flux becomes trapped in the small loop enclosed by the two junctions. However, the difference in area, and therefore in self inductance, between this small loop and the main washer loop is so large that we feel this is unlikely. It would be worthwhile to repeat the measurements using a ring

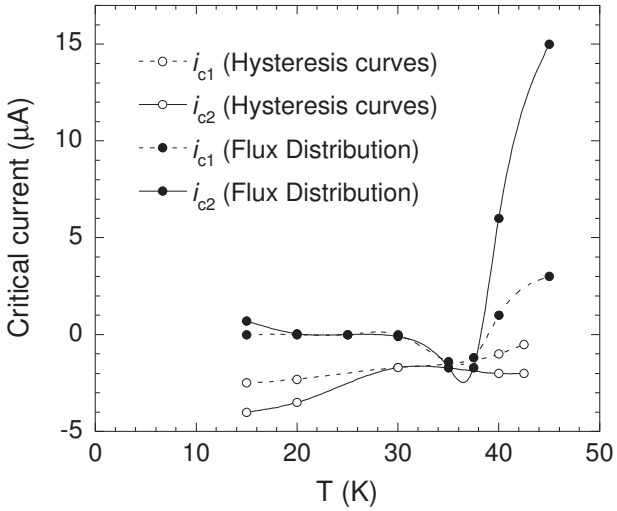

Figure 7. Temperature dependence of the values of I_{c1} and I_{c2} obtained from simulations of the hysteresis curves and the flux distributions. The lines are a guide to the eye.

containing only one junction.

7. Conclusion

We have measured the flux hysteresis curves and the distribution of trapped flux in a thin film $YBa_2Cu_3O_7$ SQUID consisting of a large washer, interrupted by an effectively single [001]-tilt grain boundary Josephson junction with an asymmetric misorientation angle of 30°. Our measurements show striking anomalies, namely the appearance of secondary loops in the hysteresis curves and a bifurcation of the flux distribution. Both anomalies are temperature dependent.

We have modelled our results using a simple model of the flux dynamics, adapted to incorporate the effect of a possible second harmonic in the CPR. By careful choice of the parameters I_{c1}, I_{c2} and L we obtain good qualitative agreement between the data and simulations. The bifurcation in the flux distribution and the secondary loops in the hysteresis curves are both modelled well with a large negative I_{c2} and a smaller negative I_{c1}. However, at other temperatures we have been unable to find a consistent set of parameters that describe both the hysteresis curves and the flux distributions.

We conclude that we have observed tentative evidence for a temperature dependent second harmonic term in the CPR. Our results are surprising because substantial second harmonic components in the CPR have only been observed previously in grain boundary junctions with misorientation angles of 45° [11, 12]. It is expected that in such junctions the first harmonic should disappear by symmetry. However, in a 30° grain boundary junction, the first harmonic is not expected to disappear, making our observation of the second harmonic quite striking. Previous measurements made by us on a grain boundary SQUID with misorientation angle 24° revealed no evidence of a second harmonic term. However, the critical currents of the junctions in that device were so large that it was extremely difficult to suppress them enough to measure the distribution of trapped flux. Measurements by Il'ichev et al. [17] on a grain boundary SQUID with misorientation angle 36° also revealed no evidence of a second harmonic term. However, we believe that our conclusion does not contradict this, as the relative strengths of the first and second harmonic terms are likely to be governed

by many microscopic factors such as faceting, homogeneity and transparency of the grain boundary, which make every device unique.

Acknowledgments

We would like to acknowledge the work of Derek Peden and the University of Strathclyde where the devices were designed and fabricated. We also acknowledge the ESF pi-shift programme for assisting one of us (CHG) in attending EUCAS 2003. The experimental work was funded by the DTI Quantum Programme.

References

[1] Wollman D A, Van Harlingen D J, Lee W C, Ginsberg D M and Leggett A J 1993 *Phys. Rev. Lett.* **71** 2134
[2] Tsuei C C, Kirtley J R, Chi C C, Yu-Jahnes Lock See, Gupta A, Shaw T, Sun J Z and Ketchen M B 1994 *Phys. Rev. Lett.* **73** 593
[3] Kirtley J R, Tsuei C C, Sun J Z, Chi C C, Yu-Jahnes Lock See, Gupta A, Rupp M and Ketchen M B 1995 *Nature* **373** 225
[4] Wollman D A, Van Harlingen D J, Giapintzakis J and Ginsberg D M 1995 *Phys. Rev. Lett.* **74** 797
[5] Miller J H Jr, Ying Q Y, Zou Z G, Fan N Q, Xu J H, Davis M F and Wolfe J C 1995 *Phys. Rev. Lett.* **74** 2347
[6] Brawner D A and Ott H R 1996 *Phys. Rev. B* **53** 8249
[7] Sigrist M and Rice T M 1992 *J. Phys. Soc. Jpn.* **61** 4283
[8] Zhang W 1995 *Phys. Rev. B* **52** 3772
[9] Tanaka Y and Kashiwaya S 1996 *Phys. Rev. B* **53** R11957
[10] Hilgenkamp H and Mannhart J 2002 *Rev. Mod. Phys.* **74** 485
[11] Il'ichev E, Zakosarenko V, IJsselsteijn R P J, Schultze V, Meyer H-G and Hoenig H E 1998 *Phys. Rev. Lett.* **81** 894
[12] Il'ichev E, Grajcar M, Hlubina R, IJsselsteijn R P J, Hoenig H E, Meyer H-G, Golubov A, Amin M H S, Zagoskin A M, Omelyanchouk A N and Kupriyanov M Yu 2001 *Phys. Rev. Lett.* **86** 5369
[13] Gallop J C, Hao L and Reed R P 1998 *J. Appl. Supercond.* **5** 285
[14] Lee R A M, Hao L, Peden D A, Gallop J C, Macfarlane J C and Roman E J 2001 *IEEE Trans. Appl. Supercondt.* **11** 859
[15] Copetti C A, Rüders F, Oelze B, Buchal Ch, Kabius B and Seo J W 1995 *Physica C* **253** 63
[16] Gallop J C 1991 "SQUIDs, the Josephson Effects and Superconducting Electronics" (Adam Hilger, Bristol, Philadelphia and New York), p24
[17] Il'ichev E, Zakosarenko V, IJsselsteijn R P J, Hoenig H E, Schultze V, and Meyer H-G 1999 *Phys. Rev. B* **60** 3096